FISEVIER

Contents lists available at ScienceDirect

## Journal of Hydrology: Regional Studies

journal homepage: www.elsevier.com/locate/ejrh



# Reconstruction of long-term hydrologic change and typhoon-induced flood events over the entire island of Taiwan

Jac Stelly <sup>a</sup>, Yadu Pokhrel <sup>a,\*</sup>, Amar Deep Tiwari <sup>a</sup>, Huy Dang <sup>a</sup>, Min-Hui Lo <sup>b</sup>, Dai Yamazaki <sup>c</sup>, Tsung-Yu Lee <sup>d</sup>

- <sup>a</sup> Department of Civil and Environmental Engineering, Michigan State University, East Lansing, MI, United States
- <sup>b</sup> Department of Atmospheric Sciences, National Taiwan University, Taipei, Taiwan
- <sup>c</sup> Institute of Industrial Science, University of Tokyo, Tokyo, Japan
- <sup>d</sup> Department of Geography, National Taiwan Normal University, Taipei, Taiwan

#### ARTICLE INFO

#### Keywords: Hydrodynamics Typhoon Floods Modeling Taiwan Climate change

#### ABSTRACT

Study region: The island of Taiwan.

Study focus: This study presents long-term and high-resolution modeling of flood occurrence, interdecadal patterns of river-floodplain dynamics, and analysis of flooding during two typhoon events-Nari and Morakot over Taiwan. The modeling system combines a hydrological model (HiGW-MAT) and a river hydrodynamics model (CaMa-Flood), simulating hydrologichydrodynamic processes at  $\sim 5$  km resolution with flood occurrences downscaled to  $\sim 90$  m. New hydrological insights for the region: As the first investigation to conduct spatially comprehensive and temporally continuous modeling in Taiwan, this study presents important advances on the application of large-scale hydrological-hydrodynamic models in settings like that of Taiwan with important implications on flood prediction under climate change. The assessment of interdecadal changes in streamflow indicates no consistent trends over the past four decades; however, the variabilities in monthly-scale streamflow are significant and regionally diverse across Taiwan. Decadal changes in flood occurrence are also minimal at the island-scale, but the changes vary substantially across different regions and exhibit an increased variability over time. Furthermore, the simulated flood patterns in response to Typhoons Nari and Morakot suggest that the modeling framework can be used to reproduce the spatial dynamics and temporal progression of flooding under extreme events in relatively small regions like Taiwan.

#### 1. Introduction

Climate change has intensified the global hydrological cycle, and this has led to an increasing frequency and severity of extreme hydroclimatic events which adversely affects water resource planning and management (Gudmundsson et al., 2021; Huntington, 2006; IPCC, 2021). Since the middle of the last century, regions throughout the world have experienced an increase in heavy rainfall events over concentrated periods of time (Bertilsson et al., 2019; Ghosh et al., 2019) that have led to record-breaking floods (Apurv et al., 2015; Li et al., 2023; Payne et al., 2020; Ripple et al., 2022). Throughout the same period, many other regions have suffered from extended dry periods and historic droughts (King et al., 2020; Liu et al., 2023), and a projected future warming (Hirabayashi et al.,

E-mail address: ypokhrel@msu.edu (Y. Pokhrel).

<sup>\*</sup> Corresponding author.

2021; IPCC, 2021) is likely to further increase the frequency of these hydroclimatic extremes (Alifu et al., 2022; Pokhrel et al., 2021; Satoh et al., 2022). The impact of these intensified extremes will vary greatly across regions of diverse geographic and climatic conditions.

The island of Taiwan is among the global regions experiencing a disproportionate increase in the risk of climatic extremes due to climate change (Chen et al., 2021; Lee et al., 2020; Patz et al., 2005). Located in the latitudinal zone of high tropical cyclone activity, Taiwan is naturally predisposed to extreme periods of rainfall and drought. The region experiences, on average, two to four seasonal typhoons per year (Hung et al., 2020), which provide the majority of the island's freshwater (Cheng and Liao, 2011). However, with the continued intensification of the global hydrological cycle, the dynamics of tropical storms in this region has been changing, leading to increased typhoons in some years that cause overwhelming floods (Wei, Li, et al., 2016) or no typhoons in some years that lead to historic droughts (Kuo, 2019).

While there is a substantial amount of research on the changing patterns and impacts of typhoons in Taiwan, the number of studies on the region's hydrologic regime is limited. Most existing literature has focused on precipitation including forecasting techniques (Hong et al., 2015; Lee et al., 2006; Yang et al., 2015) and historical trends (Chu et al., 2014; Yu et al., 2006). Other focus areas include typhoon-induced landslides (Hölbling et al., 2015; Lin and Lin, 2015), socioeconomic risks of overwhelmed storm-surge infrastructure

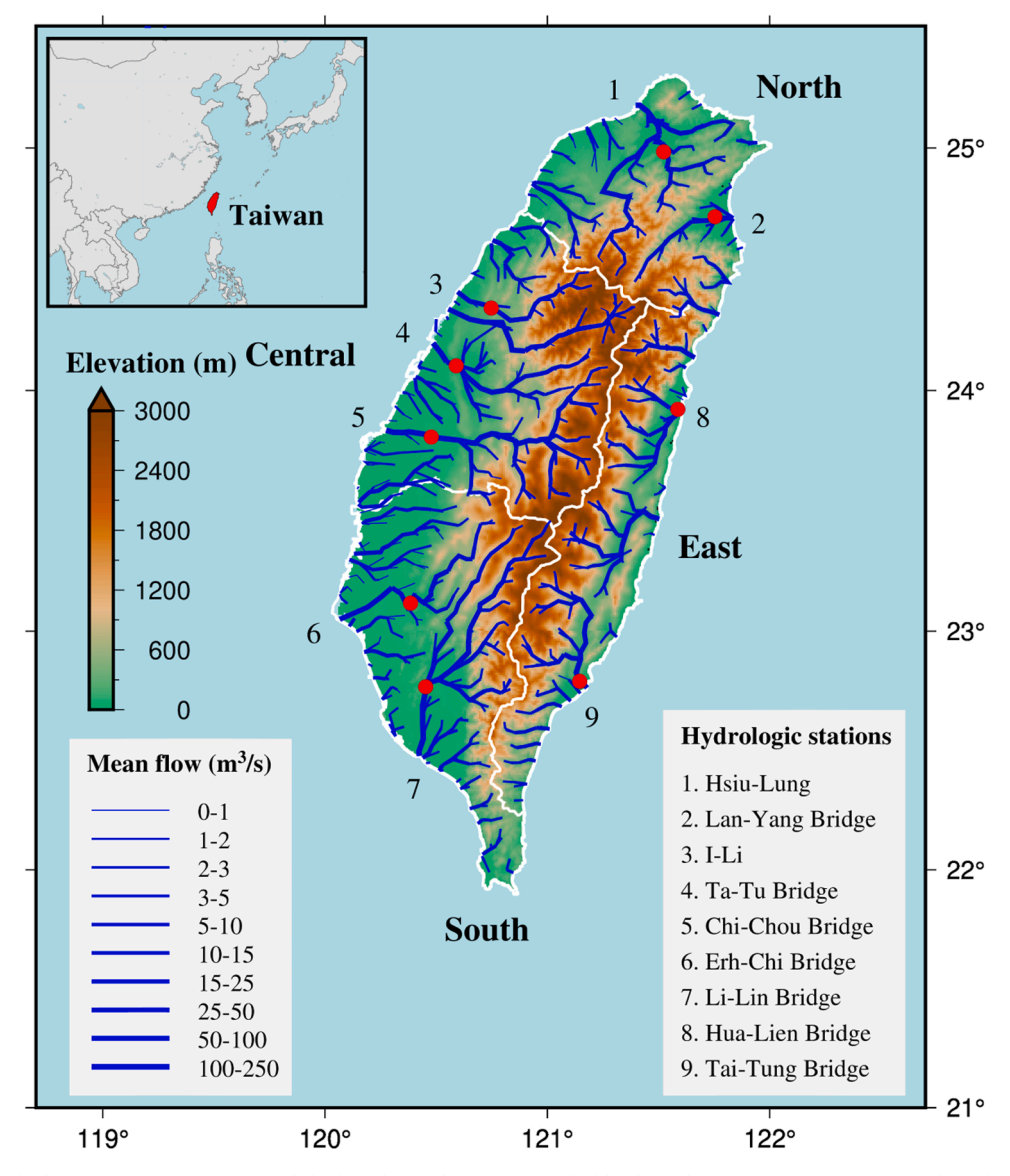


Fig. 1. The study domain – Taiwan. Background shading shows elevation (m). The blue lines depict major river networks where the line thickness represents long-term (1980–2016) daily mean flow ( $\rm m^3/s$ ) simulated by CaMa-Flood at a spatial resolution of 3-arcminute ( $\sim 5$  km). Selected hydrological monitoring stations are represented as red dots with IDs shown adjacent to the station location and full names listed at the bottom right corner. Taiwan's four main regions are named (North, Central, South, and East), and their boundaries are indicated by the white lines.

(Huang and Wang, 2015; Liu et al., 2021), and impact of typhoons on ocean wave dynamics (Hsiao et al., 2020; Shih et al., 2018). However, to the best of the authors' knowledge, there are no studies on the island-wide impacts of typhoons on streamflow and inundation occurrence in Taiwan.

Further, numerous studies have examined the hydrologic systems in Taiwan using hydrological modeling and observational data; however, these studies have focused on single watersheds or small subbasins within the island. Of the regional studies in Taiwan, the major focus is primarily on the historical impact of anthropogenic activities and/or climate change in northern (Chen et al., 2016; Lee and Yeh, 2019) and southern regions (Chen et al., 2016; Tsao et al., 2020; Yeh and Tsao, 2020), centering in watersheds relevant to major cities including Taipei, Tainan, and Kaohsiung. Further research in these regions include flood forecasting in the north (Shih et al., 2014) and south (Doong et al., 2016) and flood simulation under future climate change in the southern Tsengwen Reservoir Watershed (Kimura et al., 2014). While these studies have provided important insights on hydrologic changes in different parts of Taiwan, an understanding of the spatially complete and long-term changes in streamflow patterns and flooding is critically lacking. Existing literature includes rather limited findings, especially within the central and eastern regions of Taiwan.

Taiwan is relatively data-rich in terms of hydrological observations; however, studies utilizing streamflow from point-based measurements (Yeh et al., 2015; Yeh, 2019) are subject to limitations arising from spatial and temporal inconsistencies. The use of point-based measurements—as opposed to spatially-complete datasets—poses limits to the understanding of upstream and downstream hydrologic dynamics, and inconsistent periods of data availability as well as intermittent gaps hinder an understanding of the long-term trends and variabilities. Some studies have capitalized on the advancements in remote sensing to fill these data gaps (Chen et al., 2013; Lin et al., 2008); however, remote sensing-based data also suffers from inherent limitations, including spatio-temporal gaps caused by cloud cover and limited data periods. Further, satellite datasets have been used in hydrologic studies covering Taiwan, but they too are subject to limitations such as coarse spatial (Ji et al., 2018) or temporal (Pekel et al., 2016) resolutions, which lead to an inability to capture the short-term changes in flooding during extreme events such as typhoons.

Overall, there is a large body of literature on hydroclimatic changes in Taiwan as well as analyses for water resource applications; however, critical gaps remain as noted above. Here, we address these gaps by presenting comprehensive analyses of the decadal-scale and spatially comprehensive changes in hydrologic and hydrodynamic systems. We ask the following science questions. Could large-scale hydrologic-hydrodynamic models be used to simulate streamflow and flood dynamics in a highly complex hydroclimatic and topographic setting like Taiwan? Can such models reproduce hydrologic extremes such as floods during high-intensity typhoons? How has Taiwan's hydrology evolved in the past four decades under climate change and variability? The research objectives are to (i) demonstrate the first application of island-level hydrologic-hydrodynamic modeling for Taiwan, (ii) reconstruct the evolution of Taiwan's hydrology over the last four decades, and (iii) examine the models' ability to reproduce flood occurrence during two major historical typhoon events, namely Nari-2001 and Morakot-2009. To this end, we employ a modeling framework that combines an advanced land surface model called HiGW-MAT (Pokhrel et al., 2015, 2018a, 2018b, 2018c) with a state-of-the-art global hydrodynamic model called the CaMa-Flood (Yamazaki et al., 2011, 2013, 2014). This framework provides a computationally optimal modeling system for process-based simulations of land hydrology at a relatively coarser grid (i.e., HiGW-MAT) and river-floodplain hydrodynamics at a high resolution (i.e., CaMa-Flood). The outcomes include spatially complete and temporally continuous results of changes in streamflow and floods, allowing us to resolve the inconsistencies or gaps in observed data while also providing model validation to support future studies as climate change continues to effect global hydrology.

## 2. Study area

The study area is the entire island of Taiwan (Fig. 1), located in East Asia and bordered by various bodies of water: the East China Sea to the north, the Philippine Sea to the east, the Luzon Strait to the direct south, and the South China Sea on its southwest side. Due to large part of its direct exposure to the Pacific Ocean, Taiwan experiences volatile winds, waves, and an average annual rainfall of 2500 mm, amounting to almost three times the global average (Chen et al., 2016). A total of 80 % of this average annual rainfall occurs between May and October with low rainfall during the rest of the year (Cheng and Liao, 2011; Wei, Yeh, et al., 2016) making the island reliant on typhoon activity for freshwater resources.

Compounding the effects of the region's high degree of rainfall seasonality, Taiwan is located along an active orogenic belt at the convergence of the Eurasian and Philippines sea plates (Tang et al., 2019). The resulting central mountain range of Taiwan has a footprint of roughly 20,000 km², accounting for more than half of Taiwan's total land area of 36,000 km², with over 250 peaks reaching an elevation of over 3000 m (Fang et al., 2011). The steep topography of Taiwan's Central Mountain Range allows monsoon rain to run off rapidly, causing flooding and landslides in downstream areas during the wet season (Yeh et al., 2015), while also limiting natural buffer capacity for dry season water supply (Yen and Chen, 2001). Therefore, despite its high average annual rainfall, Taiwan's high variability of elevation and precipitation over space and time makes water resource management in the region notoriously challenging (Yeh, 2019).

These unique geographic characteristics influence the anthropological development of the island as well. Land cover in Taiwan is predominantly dense vegetation (58.9 %) with cultivated cropland (16.0 %), sparse vegetation (14.2 %), urban development (9.4 %), and wetlands (1.5 %) (Abdulmana et al., 2021). As a result, a large fraction of the 23 million resident population and associated socioeconomic activities are centered in low-lying coastal regions. This exposes urban areas, farming communities, and industrial centers to high risk of flooding. These risks substantially impact not only Taiwanese society but also the global economy. For example, disruptions in water supplies for the high-tech manufacturing industries in Taiwan, particularly in the semiconductor sector (Huang et al., 2001; Rasiah et al., 2016), can have significant repercussions on worldwide industrial supply chains (Contractor and Kundu, 2004; Ourbak and Magnan, 2018). Therefore, it is increasingly important to better understand how climate change is reshaping the

hydrological landscape in Taiwan and the resulting impacts on river flow (i.e., water resources) and inundation dynamics (i.e., flood risk).

Among the many high-intensity typhoons that have struck Taiwan since the year 2000, notable examples include Typhoon Nari (September 2001) and Typhoon Morakot (August 2009). In September of 2001, Typhoon Nari caused an effective rainfall of over 1400 mm, over 100 casualties, and an estimated US\$140 million in agricultural damage (Yang et al., 2008). Rainfall began in the northern regions of the island near Taipei, and as the storm progressed, it migrated south. The 3-day rainfall accumulation peaks totaled to  $\sim$  1431 mm roughly 50 km south of Taipei and 1241 mm near Chiayi City (Yang et al., 2008). In August of 2009, Typhoon Morakot brought even more torrential rains compared to Nari. Cumulative rainfall reached nearly 3000 mm with a maximum intensity of 109.5 mm/h which caused over 750 casualties, 1.5 million houses without power, and US\$535 million in total damages (Chen et al., 2019).

## 3. Methods and data

#### 3.1. Model description and simulation settings

CaMa-Flood (Yamazaki et al., 2011, 2012) is a global hydrodynamic model that has been widely adopted in both global and regional scale studies (Alifu et al., 2022; Chaudhari and Pokhrel, 2022; Hirabayashi et al., 2013; Pokhrel et al., 2018a, 2018b, 2018c; Yamazaki et al., 2012) due to its ability in simulating realistic river-floodplain hydrodynamics properties. The model was developed using the unit catchments concept (Yamazaki et al., 2011), where each unit has discretized river and floodplain topography parameters to better present subgrid-scale processes. This is particularly beneficial in the simulation of flood depth (floodplain inundation depth) allowing for enhanced analysis of fluvial flooding especially in regions of highly seasonal precipitation. Water storage and river streamflow are prognostic variables (Yamazaki et al., 2013) used to compute other hydrodynamics variables from upstream to downstream units. First, water level and flood depth are calculated from water storage in each unit catchment based on the discretized parameters based on MERIT Hydro dataset (Yamazaki et al., 2019). This study uses the default parameters of CaMa-Flood (Yamazaki et al., 2019) to expand the understanding of base-level performance and further enable future studies to apply the model in new ways. Then, the local inertial equation is applied to calculate river streamflow at each unit catchment. Lastly, local runoff and streamflow (both inflow and outflow) of each unit are accounted for in a mass conservation equation to update its water storage value at the next time-step. Additional information regarding the details of CaMa-Flood's physics representation, parameterization methods, or other input parameters can be found in previous literature on model description (Yamazaki et al., 2011, 2013, 2014).

Daily simulated runoff from HiGW-MAT model (Pokhrel et al., 2015) is used as the only external input to drive CaMa-Flood simulation. Based on the MATSIRO land surface model (Takata et al., 2003), HiGW-MAT is a global hydrological model that is capable of modeling evapotranspiration, infiltration, irrigation, flow regulation, and groundwater pumping on a full physical basis. Since the aims of this study are to analyze the long-term historical hydrodynamic changes and replicate natural flood conditions of short-term extreme events, anthropogenic activities are disabled within both HiGW-MAT and CaMa-Flood simulation. This study expands upon the validation of HiGW-MAT in the previous literature (Pokhrel et al., 2012, 2015, 2016; Takata et al., 2003) and broadens its application. It should be noted that CaMa-Flood can also be driven by other runoff datasets at varying resolutions such as those from the ECMWF Reanalysis v5 (ERA5) (Hersbach et al., 2020), Phase 6 of the Coupled Model Intercomparison Project (CMIP6) (Eyring et al., 2016), or the Inter-Sectoral Impact Model Intercomparison Project (ISIMIP) (Warszawski et al., 2014).

In this study, CaMa-Flood version 4.0 is used; the model is regionally set up at a spatial resolution of 3-arcminute (~ 5 km at the equator) covering all of Taiwan (21–26°N and 119–123°E; Fig. 1). Following previous studies (Pokhrel et al., 2018a, 2018b, 2018c, Shin et al., 2021, Chaudhari et al., 2022), daily runoff forcing is taken from HiGW-MAT model set up at the spatial resolution of 0.5° (~ 50 km) and driven by WATCH Forcing Data through the ERA-Interim (WFDEI) global forcing dataset (Weedon et al., 2014). The simulation period is set as 1979–2016 considering the availability of the WATCH forcing dataset. A 5-year spinup is conducted before running the model from 1979 and the first year of simulation is discarded as further spinup, thus we use the results from 1980 to 2016 (37 years) for the analyses. With the selected runoff, CaMa-Flood simulations take less than a minute for one year of simulation on a 16-core Linux computing system. The output is saved at the daily interval. Results of streamflow is used at the native CaMa-Flood resolution; however, flood depth is downscaled to a higher resolution of 3-arcsecond (~ 90 m), following previous studies (Chaudhari and Pokhrel, 2022; Dang et al., 2022; Pokhrel et al., 2018a, 2018b, 2018c; Yamazaki et al., 2014).

Flood occurrence is computed using downscaled daily flood depth to find the percentage of days in which the unit catchment is flooded. If the simulated flood depth reaches a threshold of 0.05 m, the unit catchment is assigned a value of 1. If the simulated flood depth at this location does not reach the threshold, the unit catchment is assigned a value of 0. Based upon this binary notation, a percentage of days in which flooding occurred is calculated at each location. The long-term average of this flood occurrence is validated against satellite imagery. The observed data, however, does not utilize a threshold. Instead, spectral properties of water are measured by Landsat 5 Thematic Mapper (TM), the Landsat 7 Enhanced Thematic Mapper-plus (ETM+) and the Landsat 8 Operational Land Imager (OLI) (Pekel et al., 2016). These observations are referred to as water occurrence, and the same binary notation is used to achieve a percentage of days in which water is found at a given location. Simulated flood occurrence is compared to observed water occurrence in Section 4.3. A flowchart of general methodology is presented in Fig. S1.

#### 3.2. Data

Daily observed data from hydrological monitoring stations provided by the Taiwanese Water Resource Agency are used to validate

both long-term and short-term performance of the model. Stations on nine of Taiwan's major rivers are selected as shown in Fig. 1, and all stations had a minimum observational period of 17 years during the 1980–2016 period. Additional information including station number, river name, coordinates, and temporal availability of data can be found in the Supplementary material (Table S1).

Additionally, to evaluate the simulated inundation dynamics, an archive of multi-temporal orthorectified remote sensing monthly data derived from Landsat 5, 7 and 8 at a resolution of 1-arcsecond ( $\sim$  30 m) for the period of 1984–2021 is acquired through the Joint Research Centre's Global Surface Water (GSW) dataset (Pekel et al., 2016), which provides information in terms of water presence at each grid cell within the region. The dataset is further processed into long-term average (from 1984 to 2016) water occurrence spatial map and upscaled to 3-acrsecond resolution for a consistent comparison with the downscaled simulated results of CaMa-Flood.

#### 4. Results

## 4.1. Validation of Streamflow

The HiGW-MAT and CaMa-Flood combination of modeling framework has been validated in previous studies globally (Zhao et al., 2017) as well as for some of the world's most prominent regions including the Mekong River basin (Dang et al., 2022; Pokhrel et al., 2018a, 2018b, 2018c; Shin et al., 2020a, 2020b), Amazon River basin (Chaudhari and Pokhrel, 2022), Itajaí-Açu River Basin of southern Brazil (Fleischmann et al., 2019), and the Himalayan region (Shin et al., 2021). However, because this is the first application of the model in Taiwan, we present an evaluation of simulated results at the nine hydrological monitoring stations located in major river basins across Taiwan (Fig. 1). We specifically assess the model performance by comparing the seasonal cycle of the long-term (1980–2016) average of simulated streamflow (Fig. 2) and water level anomaly (Fig. S2) against observed data at each station. Fig. 2 shows the comparison between observed and simulated monthly streamflow along with model performance indicators including the coefficient of determination ( $R^2$ ), percent bias (pBIAS), and Kling-Gupta Efficiency (KGE; Gupta et al., 2009). The  $R^2$  values higher than 0.9. Moreover, the comparison based on percent bias also shows good model fidelity at stations 4 and 9 showing a pBIAS of < 5 %. Stations 3 and 5 both display a marginal overestimation of streamflow; nonetheless, all other stations achieved a pBIAS value of less than  $\pm$  25 %. Ranging from negative infinity to one, KGE values of over - 0.41 constitute a reasonable model (Knoben et al., 2019), and all stations in this study achieved this threshold. The average KGE value at the nine stations is 0.64, and the lowest KGE (i.e.,

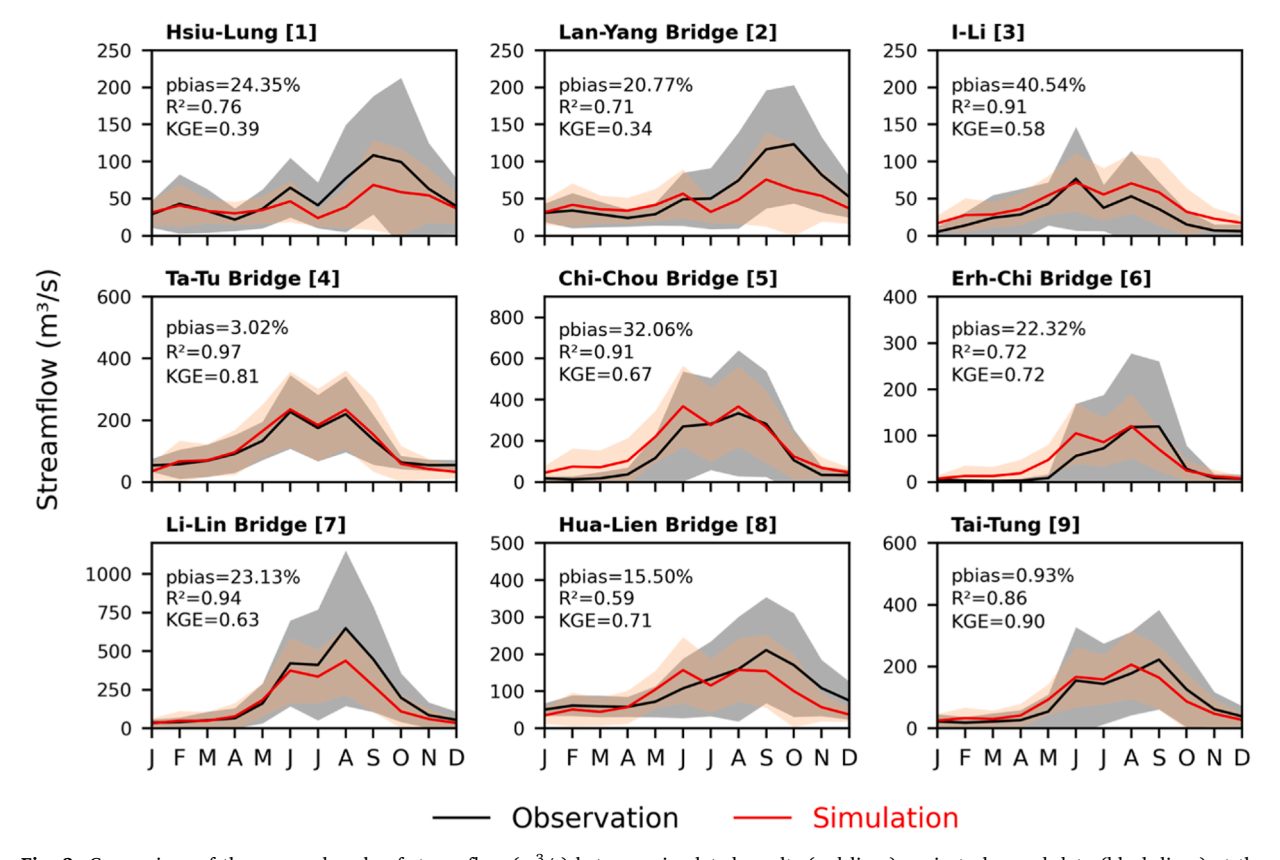


Fig. 2. Comparison of the seasonal cycle of streamflow  $(m^3/s)$  between simulated results (red lines) against observed data (black lines) at the selected locations. Shadings (light orange for simulated results and grey for observation, respectively) indicate interannual variability presented as one standard deviation for each month.  $R^2$ , pBIAS, and KGE values are indicated for each station.

0.34) is found at station 2. Moreover, high variation in the streamflow can be observed in Taiwan, especially during the wet season. In general, the model tends to underestimate streamflow in northern Taiwan (stations 1, 2) and there are minor differences at other locations in central Taiwan (stations 3–5), southern Taiwan (stations 6, 7), and eastern Taiwan (stations 8, 9). Additionally, there are certain mismatches in terms of timing for the flood season peaks at stations 6 and 8. These discrepancies could be attributed to various factors including model parameters (e.g., river width and depth) and uncertainties in forcing data. Some of the discrepancies could have also been caused by the impacts of human activities (e.g., reservoirs and water withdrawals) that are not considered in the current simulations. Recognizing these uncertainties and given that CaMa-Flood is a large-scale model used over Taiwan without region-specific parameter optimization, we consider the results to be of reasonable accuracy for the objective of this study.

#### 4.2. Trends and patterns of historical streamflow

Fig. 3 presents the decadal average seasonal streamflow at each station over the course of four decades: 1980s, 1990s, 2000s, and 2010s (note that the 2010s include only seven years, 2010–2016). All stations within the central, southern, and eastern regions display a clear seasonal cycle with a wet season occurring from May to October and a dry season from November to April. Within this annual seasonality, monthly averages in each decade exhibit high and low flows in a relatively quick succession providing further evidence of the high hydrological variability of an island exposed to the Northwest Pacific Ocean. These are often caused by extreme events occurring within the decade, whether that be flooding or drought, which tends to skew the decadal average for a given month. To visualize the extreme events of each decade, daily streamflow of each year is presented in Fig. S3.

The period of highest maximum flow varied across regions; however, all stations exhibit peaks in either the 2000s or 2010s. Stations 1 and 2, located in the north, display peaks in the 2000s, however, this is followed by a substantial drop of total water volume in the 2010s which is the driest among the four decades. Streamflow pattern at these northern stations exhibit a singular peak in September which is later compared to the timing of peaks at all other stations. Results for the central region (stations 3–5) indicate the lowest maximum flow in the 1980s with an incremental progression across each decade. Peak flows in the 2000s and 2010s are relatively similar at stations 4 and 5, and at station 3, peak flow in the 2010s is the highest. In this region, peak flow occurs in both June and August. Stations 6 and 7, which are located in the southern regions, also display peaks in June and August as well as an incremental

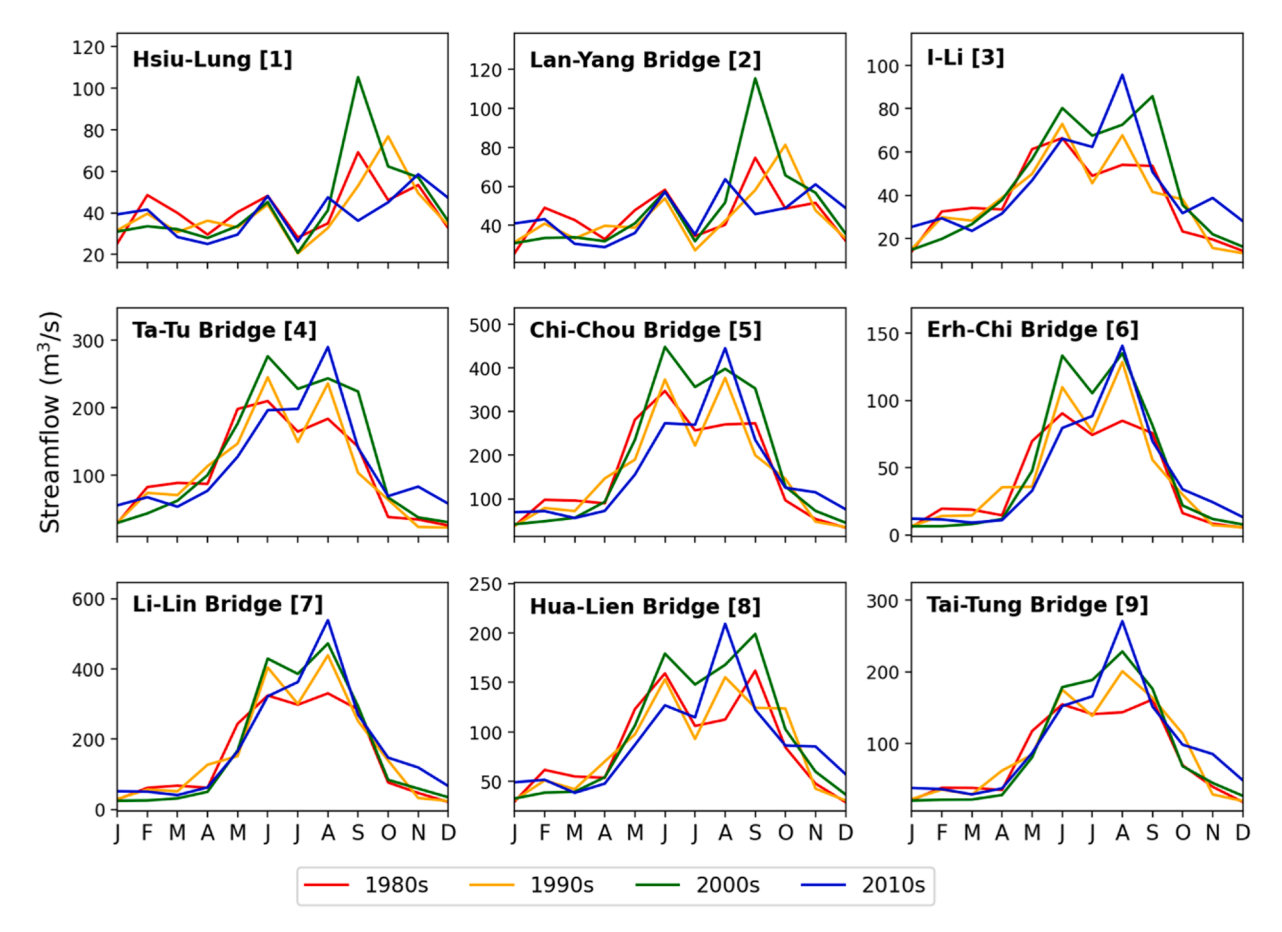


**Fig. 3.** Decadal (color-coded lines) average of monthly streamflow across four decades [1980s (1980–1989), 1990s (1990–1999), 2000s (2000–2009), and 2010s (2010–2016)] at selected locations.

progression of peak flow across all periods. Simulations at stations 8 and 9, located along the eastern coast of Taiwan, result in maximum streamflow occurring in August of the 2010s with a peak in June decreasing in relative magnitude over time. At station 8 peak flow of the 2000s and 1980s occurs in September. Total water volume is the highest in the 2000s at station 8 and in the 2010s at station 9.

It is clearly discernible in Fig. 3 that maximum (wet season) streamflow reaches 3–7 times of the minimum (dry season) streamflow for any given period. This trend is seen in small rivers such as the Da'an River assessed at station 3 as well as the Gaoping River assessed at station 7.

Overall, these results demonstrate that, (i) despite being a relatively small region, Taiwan's hydrologic regime is highly diverse with different characteristics in each of the four main regions; (ii) there has been an increasing trend in terms of volume and peak streamflow from 1980s to 2000s followed by a nonuniform drop of water volume in the 2010s; and (iii) stations in the Central, Southern, and Eastern regions of Taiwan display the highest peak flow in the 2010s. Although all the stations exhibit an increasing trend, none of them show a significant trend in streamflow during the period of 1980–2016 (Fig. S4).

#### 4.3. Evaluation of flood dynamics

Fig. 4 displays the long-term water occurrence across Taiwan for the period 1984–2016 and compares observations from the GSW dataset to results simulated by CaMa-Flood. While there are minor visible discrepancies, the broad spatial patterns of simulated flood occurrence have a good agreement with the GSW data for most of the selected sub-regions. In sub-region A (Fig. 4), the major river and floodplain is well represented in both the simulation and observation with a water occurrence of 90–100 %. Also in sub-region A, both simulations and observations capture the series of small water bodies—likely ponds—throughout the agricultural zone of Taiwan's northwest coast. In sub-region B, the inland lake/river at the top left corner of the panel is seen with high similarity between CaMa-Flood and GSW results. There are minor underestimations of the coastal areas in this panel; however, the highly saturated areas north and south of this floodplain are captured well. The most prominent discrepancies between simulation results and satellite imagery are seen in sub-region C with CaMa-Flood showing additional flooding due to overflow in floodplains of smaller rivers with minor flood

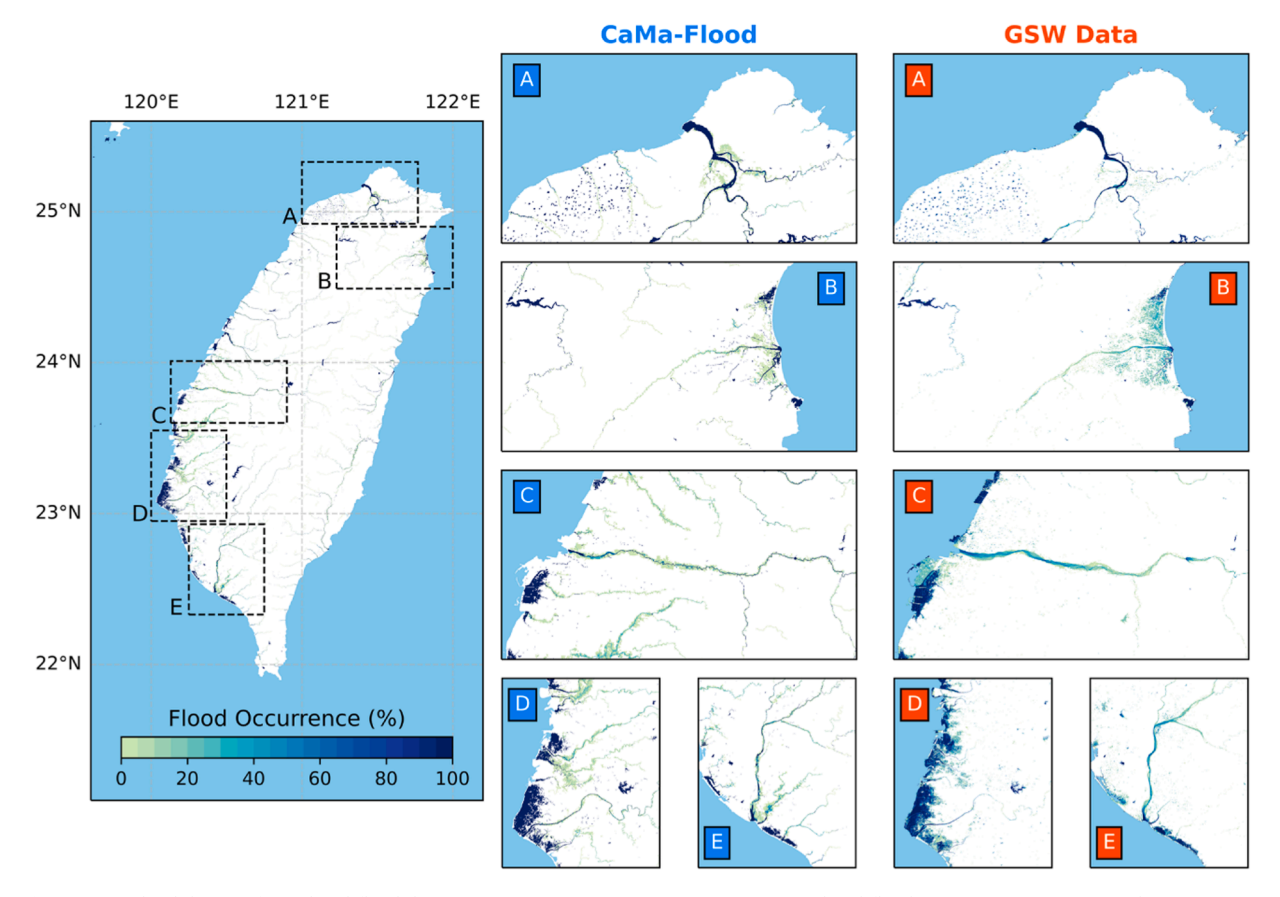
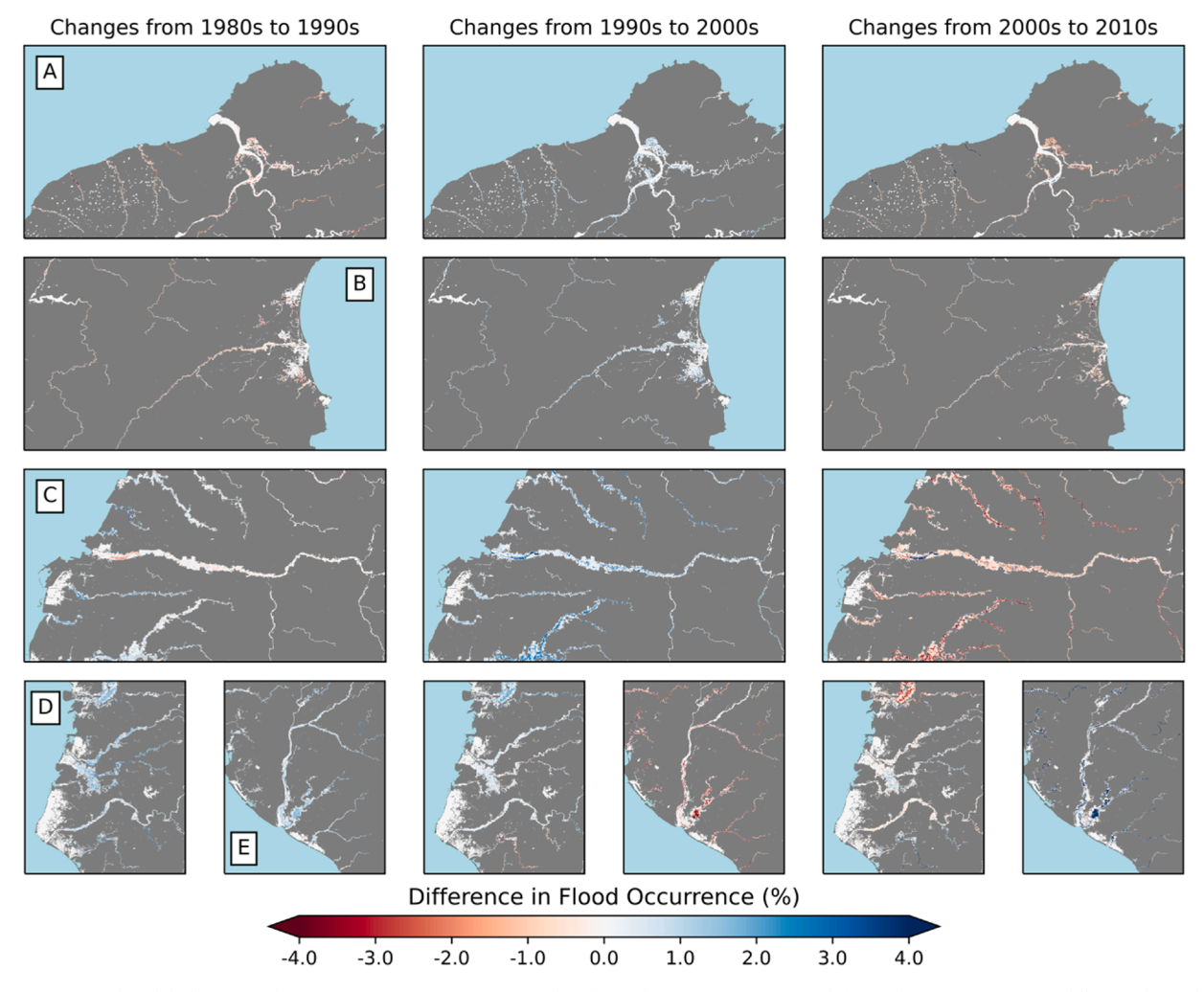


Fig. 4. Spatial validation of simulated flood dynamics. Long-term average (1984–2016) simulated flood occurrence at 3-arcsecond ( $\sim$  90 m) resolution for the entire Taiwan (left main panel). Black boxes, labeled A-E in the main panel, indicate selected sub-regions used for the comparison of flood occurrence between CaMa-Flood results (middle panels) and GSW dataset (right panels). The number of publicly available satellite images from Landsat (4–5, 7, and 8–9) used in generating the GSW dataset can be found in Table S2.

occurrence of 0-5 % ( $\sim 0-18$  days), and GSW data showing the same region with a 0 % flood occurrence. The spatial and temporal information of the major river and permanently saturated coastal zones show highly similar results. Similar to sub-region C, sub-regions D and E show highly similar representation of major rivers and heavily inundated coastal areas, and the same additional flooding of CaMa-Flood's representation of small rivers and floodplains is seen in sub-regions D and E. Additionally, for sub-regions C and D, there are certain locations in the coastal areas where simulated results could not capture the permanent flooded areas seen in the GSW data. Challenges in clearly demarking the land-ocean boundary in the model's original simulation or during the downscaling process could have resulted in this discrepancy. However, GSW data is subject to limitations due to cloud cover as well as technical issues in the water detecting method that could potentially miss flooded areas of dense vegetation or those of shallow water level. This would likely explain the 0 % water occurrence seen in the GSW dataset across the river-floodplain networks within the low-lying western river networks which are most active during wet season and extreme events with dense cloud cover.

In general, there is a high similarity between observational water occurrence and simulated flood occurrence across Taiwan. Temporal dynamics of inundation is confirmed by the similarity in percentage of days experiencing water occurrence. Spatial dynamics of the model's Digital Elevation Map (DEM) and river routing are validated by the highly similar locations of permanent and seasonal bodies of water. Areas of long-term inundation are presented with high correlation between simulation and observational results such as major rivers, coastal floodplains, and small irrigation ponds in agricultural regions. Minor differences of 0–5 % are seen in small river-floodplain systems. Considering the known difficulties of hydrodynamic simulation and the CaMa-Flood's more typical application of large-scale watershed systems, these are considered sufficiently accurate results to reconstruct historical changes in spatial inundation and examine the impact of Typhoons Nari and Morakot.



**Fig. 5.** Interdecadal change in flood occurrence (in %) from one decade to the next: 1980–1990s (left panels), 1990–2000s (middle panels) and 2000–2010s (right panels). Areas highlighted in red represent a decrease in flood occurrence; areas highlighted in blue represent an increase in flood occurrence; and areas with no flood occurrence are indicated in grey. Areas that experience flood occurrence without interdecadal change are indicated in white. The location of sub-regions from A to E are shown in Fig. 4 (left main panel).

#### 4.4. Trends and patterns of historical inundation

Fig. 5 shows the percent change in flood occurrence at selected locations in Taiwan (Fig. 4) between the 1980–1990s, 1990–2000s, and 2000–2010s, respectively. Percent change is the difference in percentage of flooded days at each unit catchment between the two periods (e.g., change from 1980s to 1990s is found by subtracting average flood occurrence of the 1980s from the average flood occurrence of the 1990s). As such, percent change represents the change in number of days, with 1 % change being equivalent to 3.65 days in terms of annual average and 4 % being equivalent to over 2.5 weeks.

Sub-region A, which includes Taipei city and the Tamsui River, experiences relatively consistent flood occurrence throughout the entire period (1980–2016) with only  $\sim 1$  % of changes between the decades and no visible monotonous trend. Region B, which includes Yilan County and the Lanyang River, exhibits rather similar flood occurrence changes as for sub-region A, which corroborates the streamflow trends seen in Fig. 3 at stations 1 and 2 respectively.

In sub-region C, the 1980s and 1990s are shown to be relatively consistent with a decrease of roughly 1 % in the Jhuoshuei River and an increase of equal magnitude to the surrounding rivers and tributaries. From the 1990s to the 2000s, all rivers exhibit a visible change amounting to a 2–3 % increase in flood occurrence. From the 2000s to the 2010s, all rivers experience a decrease, and the most notable change can be seen in the upstream areas of smaller rivers decreasing by  $\sim$  4 %, which directly aligns with results seen in Fig. 3 at station 5.

Sub-region D, corresponding to station 6 in Fig. 3, displays visible increase across all rivers in that region from the 1980s and 1990s.

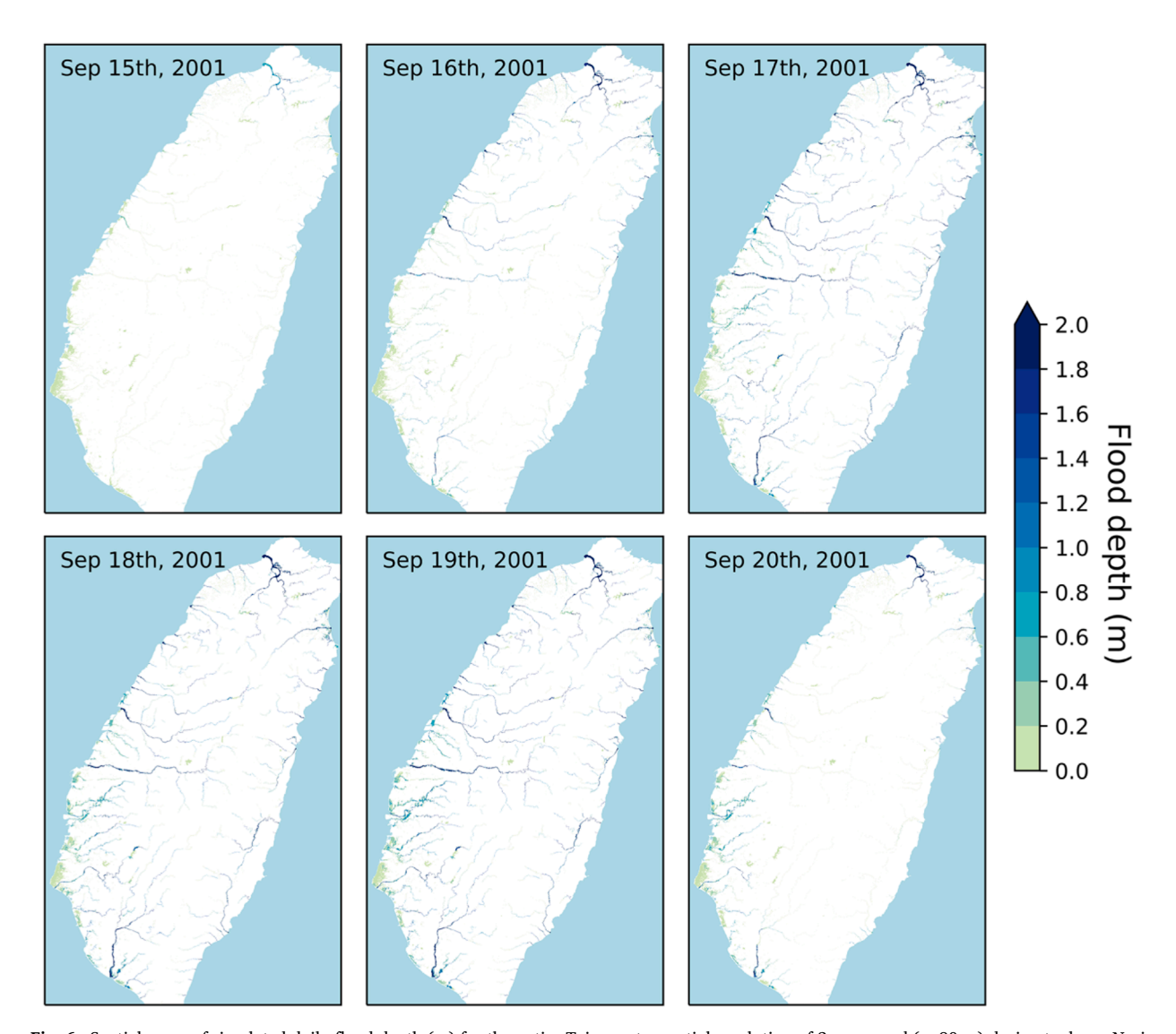


Fig. 6. Spatial maps of simulated daily flood depth (m) for the entire Taiwan at a spatial resolution of 3-arcsecond ( $\sim$  90 m) during typhoon Nari (Sep 15–20th, 2001). High-resolution animations can be found online (see data availability section). Spatial maps focusing on the western coast of Taiwan can be found in the supplementary section (Fig. S8).

This includes an increase by 2 % of larger floodplains and an increase by 4 % in certain rivers. From the 1990s to 2000s, sub-region D remains relatively consistent showing both increases and decreases by 2 % and 3 % in rivers and floodplains throughout the region. From the 2000s to 2010s, increases and decreases by 2 % and 3 % can be seen throughout the region, and there is a decrease by at least 4 % in a northern floodplain that experienced a 2 % increase in both progressions of 1980–1990s and 1990–2000s. The saturated coastline seen at nearly 100 % in Fig. 4d displays little to no change in Fig. 5 meaning the percent change of this area is within  $\pm$  0.5 % (0–2 days).

Sub-region E includes the Gaoping River, one of Taiwan's most substantial rivers in terms of streamflow, where flood occurrence can be seen increasing by  $\sim 2$ % between the 1980s and 1990s, decreasing between 1990s and 2000s by at least 4%, and increasing again between the 2000s and 2010 s by 4% or higher. Between the 1980–1990s as well as between the 2000s and 2010s, the percentage increase in water occurrence is analogous to the increase in wet season streamflow seen at station 6 and 7 (Fig. 3). The percent decrease in water occurrence between the 1990s and 2000s can be attributed to a decrease in dry season streamflow also seen at station 6 and 7 (Fig. 3).

The eastern coast of Taiwan experiences no change greater than 1 % throughout the total period (see Supplementary information; Fig. S5), which can be explained by two primary factors. First, as seen in Fig. 1, there are minimal floodplains south of Yilan county. And second, due to the steep grade of Taiwanese topography, water flows quickly from high elevation rivers into the ocean resulting in a small percentage of days in which water accumulates along the eastern coast. This can also be seen in the long-term water occurrence simulated and validated in Fig. 4.

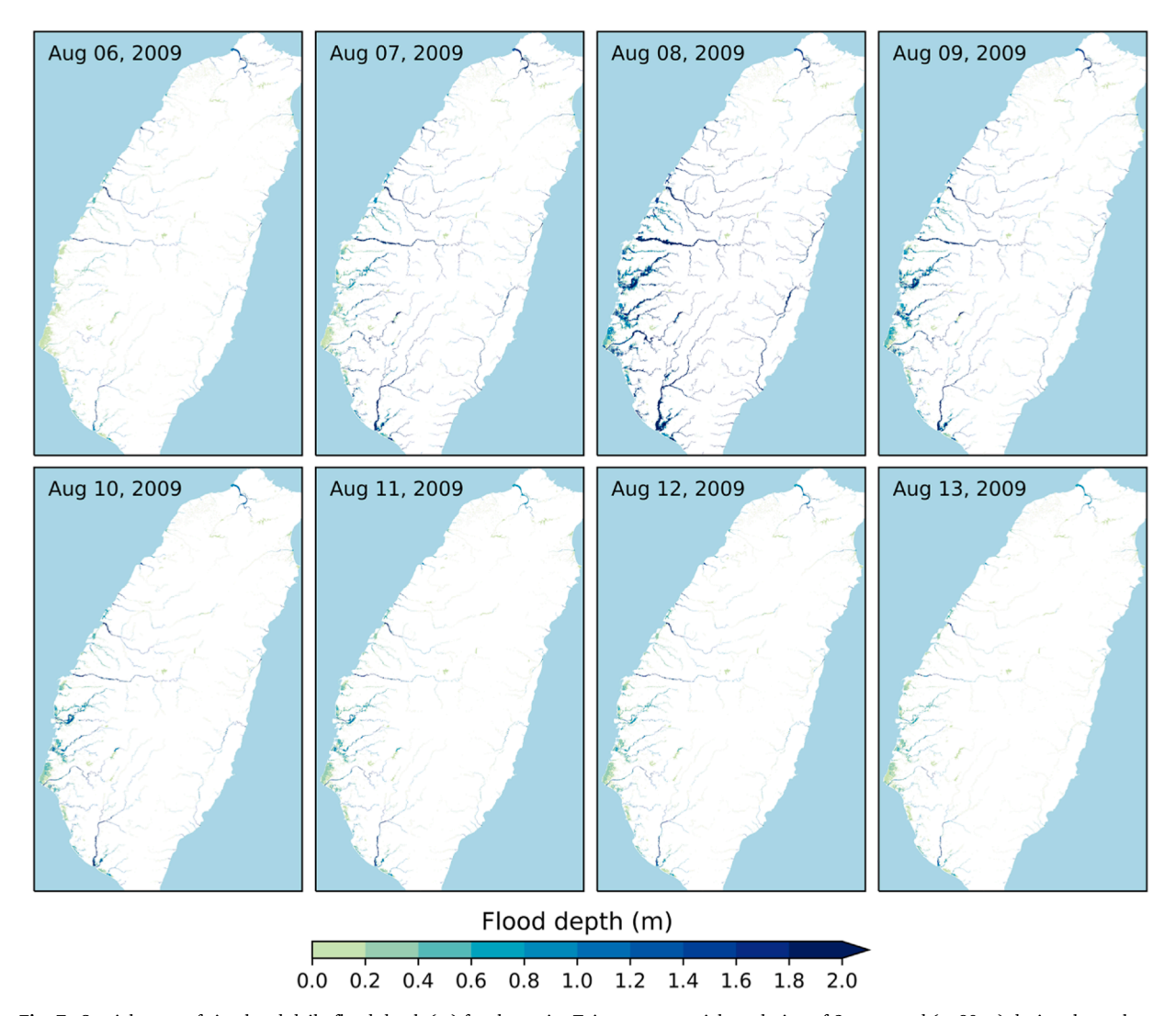


Fig. 7. Spatial maps of simulated daily flood depth (m) for the entire Taiwan at a spatial resolution of 3-arcsecond ( $\sim$  90 m) during the typhoon Morakot event (Aug 6–13th, 2009). High-resolution animations can be found online (see data availability section). Spatial maps focusing on the western coast of Taiwan can be found in the supplementary section (Fig. S9).

#### 4.5. Flood dynamics during Typhoons Nari and Morakot

Fig. 6 and Fig. 7 show the simulated daily flood depth at a  $\sim$  90 m resolution during Typhoons Nari and Morakot, respectively. Comparisons of daily simulated and observed water surface elevation anomaly throughout the duration of each typhoon are also included in the Supplementary material (Fig. S6 and Fig. S7). The simulated results have captured the events' progression relatively well with consistent day-to-day patterns between observed and simulated across all selected stations despite marginal differences.

Fig. 6 shows the 6-day progression of flooding caused by Typhoon Nari. September 15th, 2001 is the first day of this progression, which shows relatively minimal flood occurrence prior to typhoon landfall and likely represents the base flooding level during the season. Typhoon-induced flooding begins on September 16th in the northern region of Taiwan, and between the 16th and 17th, the progression of flooding progresses south along the west coast. Significant flooding continues through the 18th and 19th at a consistent depth over the two days. During this time, flood depth in the tributaries of the major rivers ranges from 1 to 1.4 m, and that in the major rivers is  $\sim 2$  m. On the 19th, minor increases can be seen in tributary flooding. On September 20th, simulations show flood depth returning to near baseline levels with some residual flooding along the southwest coast.

Fig. 7 shows the 8-day progression of Typhoon Morakot. Similar to that in Fig. 6, the first day (August 6th, 2009) is presented to show relatively low level of flooding, representing the base flood depth. However, flood depths slightly higher than at the beginning of Typhoon Nari (Fig. 6) can be observed, with flooding of 1–1.5 m occurring in major rivers and flooding of 0.2–0.6 m in the tributaries of each region. From August 6th to 7th, substantial increases of flooding can be seen throughout the island, but most predominantly, change occurs in the south and central regions. Minor changes also occur along the eastern coast, and the north region stays relatively consistent. From August 7th to the 8th, a more dramatic increase occurs, again with seasonal floodplains reaching 2 m within south and central coastal areas, major rivers widening into the respective floodplains, and mountainous river networks becoming more pronounced. Flooding begins to decrease on August 9th; however, residual flooding can be seen in low-lying coastal basins until August 12th.

#### 5. Discussion

The hydrology of Taiwan is characterized by a high degree of variability also found by Yeh et al. (2015). This variability is most notably observed during the wet season (May-October), which shows high potential for extreme dry and wet events. Our results regarding no island-wide trend in streamflow change are in line with the findings of Yeh and Tsao (2020) who showed no significant trend in streamflow at four river basins (Bazhang, Zengwen, Yanshui, and Erren) in southern Taiwan. Further, Lee and Yeh (2019) found only one among six stations in Northern Taiwan with significant (increasing) trend. Moreover, our simulations show regionally diverse volume and peak patterns which are consistent with previous literature (Chen et al., 2016; Hussain et al., 2021; Tsao et al., 2020) providing evidence of Taiwan's interannual hydrological variabilities. In general, our results corroborate previous findings on the long-term trends and regional variabilities in Taiwan, and this study fills a critical knowledge gap regarding island-wide and decadal perspectives on the changes in streamflow and flood occurrence, improving our understanding of the changes in hydrology of Taiwan.

CaMa-Flood simulated flood occurrence shows a highly similar representation of major river-floodplain systems compared to satellite-driven high-resolution flood occurrence (Pekel et al., 2016). Moreover, the simulated results prove to be able to capture additional flooding regions which the GSW data cannot due to cloud cover (Shin et al., 2020a, 2020b) allowing improvements in terms of flood risk assessment for high impact regions such as urban areas, tourist destinations, and natural wetlands.

Interdecadal analysis of change in flood occurrence shows no trends consistent throughout the island (Lee and Yeh, 2019; Tsao et al., 2020; Yeh et al., 2015). While diverse regions experience various changes of flood occurrence, simulation results show the magnitude of change increasing over time (Chu et al., 2014) which has major implications for water storage and flood prevention. With regions experiencing a difference in flooding greater than two weeks period to period, preparing infrastructure for wet season, and ensuring water availability for dry season becomes increasingly difficult. With climate change effecting the magnitude and frequency of typhoons, this difficulty may continue to progress.

High-resolution daily flood depth reproductions of Typhoons Nari and Morakot correctly represent the temporal and spatial progression of each storm (Shieh et al., 2010; Tang et al., 2012; Tsou et al., 2011; Yang et al., 2008) capturing preliminary effects, landfall, and residual flooding. Furthermore, simulations also represent specific areas of impact well compared to previous literature (Hsu et al., 2011; Li et al., 2005; Sui et al., 2002; Tsou et al., 2011; Wu et al., 2014). The accuracy of storm-specific reproductions expands on the aforementioned capability of resource management application. This modeling framework in combination with its highly efficient runtime can be used to produce real-time flood forecasts, and by running multiple scenarios over a short period of time, the model can produce a range of spatially complete outcomes to inform short-term and long-term decision making. Moreover, the same framework can be utilized for analyzing projected extreme events, such as floods and droughts, facilitating a comprehensive assessment of their potential impacts.

Even though the model simulated results accurately match with the short-term and long-term observed data, the results of this study should be interpreted with understanding that limitations of hydrodynamic modeling are likely to arise such as complications due to a lack of oceanic flooding, a disregard for historical anthropogenic activities, and potential uncertainties of forcing data or model parameters. A specific limitation in this study is the selection of coarse-resolution input data. Especially in a small area such as Taiwan, available datasets at higher resolution could potentially yield higher accuracy results. However, utilizing HiGW-MAT data at a resolution of 0.5° allows this study to assess the ability of CaMa-Flood to reproduce detailed information from broad sources of data. These findings are directly relevant to climate projections which come in coarse resolution datasets (Hsu and Dirmeyer, 2023; Lehner

et al., 2019; Satoh et al., 2022) and will hopefully support future studies analyzing the potential changes to water resources in Taiwan under a multitude of climate change scenarios.

#### 6. Conclusions

This study examines the hydrologic and hydrodynamic changes in Taiwan, presenting spatially complete and temporally continuous changes in streamflow and flood occurrence over the past four decades. It also presents the daily inundation response to extreme rainfall caused by two high-intensity typhoons, namely Nari and Morakot. The study is the first in presenting outcomes derived from a global hydrodynamic model that captures the island-wide setting like that of Taiwan. Performance of the CaMa-Flood is evaluated extensively, and our finding suggests that the model can perform well over both long-term and short-term periods in capturing the region's hydrology. Comparison of simulated streamflow and water occurrence in four periods (i.e., 1980s, 1990s, 2000s, 2010s) suggest that the hydrologic system in Taiwan has not experienced consistent trends in the past four decades; however, the seasonal variabilities in monthly-scale streamflow among the four decades are found to be substantial. A comparison of the simulated flood occurrences with satellite data suggests that CaMa-Flood effectively reproduces historical flooding patterns in the major flooded regions despite the model not being specifically calibrated for the region. Further, results indicate an increasing magnitude of fluctuations over time varying across diverse regions within the island. Finally, a close examination of daily-scale flood progression during the two typhoons indicates that the model can realistically simulate the response to such extreme events. Such progression could not be validated directly owing to lack of observational data, but a comparison of simulated water surface elevation anomaly in selected locations with available observations indicate that the results are reasonably accurate.

Results of this study could contain some uncertainties and therefore must be interpreted with caution. First, even though CaMa-Flood accounts for backwater effect in low-lying areas, it simulates only river flooding, therefore the influence of coastal flooding is not accounted for. Second, the runoff data taken from global simulations might contain uncertainties, causing discrepancies in simulated streamflow and flood occurrence. And third, the current CaMa-Flood model is simulated with global parameter settings without explicit tuning for the study region, which may have introduced further uncertainties in the outcomes. Further studies could address these limitations by using higher resolution climate forcing data, integrating the model with coastal flooding models for improved coastal flood simulations, and enhancing CaMa-Flood parameterizations by using local datasets. In conjunction with these adjustments, considering human activities (e.g., reservoir operation) could be key in improving the accuracy of short-term events such as typhoons.

Despite these limitations, this study demonstrates that a combination of large-scale land surface model and river hydrodynamics model can be used to reconstruct the hydrologic and hydrodynamic characteristics in regions such as Taiwan. More importantly, the study shows that the modeling system could be used to reproduce flooding caused by extreme precipitation events, which also implies that the model could be used to better predict extreme flooding events under varying projections of climate change. The computationally efficient modeling framework presented here could be used for such predictions at the decadal and century scales as well, which have important implications on the improved understanding of flood risk and water resource management in Taiwan under an intensifying climate.

#### Data availability

High-resolution animations of outcomes seen in Fig. 6 and Fig. 7 are available at https://doi.org/10.6084/m9.figshare.23511843.v2. Data can be made available upon request to authors.

#### CRediT authorship contribution statement

Min-Hui Lo: Writing – review & editing, Resources, Methodology, Data curation. Huy Dang: Writing – review & editing, Visualization, Validation, Software, Methodology, Investigation, Funding acquisition, Formal analysis. Dai Yamazaki: Writing – review & editing, Software, Methodology. Tsung-Yu Lee: Writing – review & editing, Methodology, Data curation. Jac Stelly: Writing – review & editing, Writing – original draft, Visualization, Validation, Software, Methodology, Investigation, Formal analysis, Conceptualization. Amar Deep Tiwari: Writing – review & editing, Visualization, Validation, Software, Methodology, Investigation, Formal analysis. Yadu Pokhrel: Writing – review & editing, Writing – original draft, Supervision, Resources, Project administration, Methodology, Investigation, Funding acquisition, Conceptualization.

#### **Declaration of Competing Interest**

The authors declare that they have no known competing financial interests or personal relationships that could have appeared to influence the work reported in this paper.

## Data availability

Data will be made available on request.

#### Acknowledgements

Yadu Pokhrel gratefully acknowledges financial support for this research by the Fulbright U.S. Scholar Program, which is sponsored by the U.S. Department of State and Foundation for Scholarly Exchange (FSE), Taiwan. Its contents are solely the responsibility of the author and do not necessarily represent the official views of the Fulbright Program, the Government of the United States, or FSE. This study was also partially supported by the National Science Foundation (Awards #: 1752729 and 2127643).

## Appendix A. Supporting information

Supplementary data associated with this article can be found in the online version at doi:10.1016/j.ejrh.2024.101806.

#### References

- Abdulmana, S., Lim, A., Wongsai, S., Wongsai, N., 2021. Land surface temperature and vegetation cover changes and their relationships in Taiwan from 2000 to 2020. Remote Sens. Appl.: Soc. Environ. 24, 100636 https://doi.org/10.1016/J.RSASE.2021.100636.
- Alifu, H., Hirabayashi, Y., Imada, Y., Shiogama, H., 2022. Enhancement of river flooding due to global warming. Sci. Rep. 12 (1) https://doi.org/10.1038/s41598-022-25182-6.
- Apurv, T., Mehrotra, R., Sharma, A., Goyal, M.K., Dutta, S., 2015. Impact of climate change on floods in the Brahmaputra basin using CMIP5 decadal predictions. J. Hydrol. 527 https://doi.org/10.1016/j.jhydrol.2015.04.056.
- Bertilsson, L., Wiklund, K., de Moura Tebaldi, I., Rezende, O.M., Veról, A.P., Miguez, M.G., 2019. Urban flood resilience a multi-criteria index to integrate flood resilience into urban planning. J. Hydrol. 573 https://doi.org/10.1016/j.jhydrol.2018.06.052.
- Chaudhari, S., Pokhrel, Y., 2022. Alteration of river flow and flood dynamics by existing and planned hydropower dams in the Amazon River Basin. Water Resour. Res. 58 (5) https://doi.org/10.1029/2021WR030555.
- Chen, Y.-J., Chu, J.-L., Tung, C.-P., Yeh, K.C., Chen, C., Chu, J.L., Tung, C.P., Yeh, K.C., 2016. Climate change impacts on streamflow in Taiwan catchments based on statistical downscaling data. Terr. Atmos. Ocean. Sci. 27 (5), 741–755. https://doi.org/10.3319/TAO.2016.07.20.01.
- Chen, S., Hong, Y., Cao, Q., Kirstetter, P.E., Gourley, J.J., Qi, Y., Zhang, J., Howard, K., Hu, J., Wang, J., 2013. Performance evaluation of radar and satellite rainfalls for Typhoon Morakot over Taiwan: are remote-sensing products ready for gauge denial scenario of extreme events? J. Hydrol. 506, 4–13. https://doi.org/10.1016/J.JHYDROL.2012.12.026.
- Chen, Y.-S., Tsai, Y.-J., Shieh, C.-L., Wang, C.-M., Tseng, W.-H., 2019. An overview of disasters resulted from Typhoon Morakot in Taiwan. (https://www.researchgate.net/publication/285977880).
- Chen, C.C., Wang, Y.R., Wang, Y.C., Lin, S.L., Chen, C.T., Lu, M.M., Guo, Y.L.L., 2021. Projection of future temperature extremes, related mortality, and adaptation due to climate and population changes in Taiwan. Sci. Total Environ. 760 https://doi.org/10.1016/j.scitotenv.2020.143373.
- Cheng, C.-L., Liao, W.-J., 2011. Current Situation and Sustainability of Water Resource in Taiwan. Asian Water Saving Council.
- Chu, P.S., Chen, D.J., Lin, P.L., 2014. Trends in precipitation extremes during the typhoon season in Taiwan over the last 60 years. Atmos. Sci. Lett. 15 (1) https://doi.org/10.1002/asl2.464.
- Contractor, F.J., Kundu, S., 2004. The role of export-driven entrepreneurship in economic development: a comparison of software exports from India, China, and Taiwan. Technol. Forecast. Soc. Change 71 (8 SPEC. ISS.). https://doi.org/10.1016/j.techfore.2004.01.012.
- Dang, H., Pokhrel, Y., Shin, S., Stelly, J., Ahlquist, D., Du Bui, D., 2022. Hydrologic balance and inundation dynamics of Southeast Asia's largest inland lake altered by hydropower dams in the Mekong River basin. Sci. Total Environ. 831 https://doi.org/10.1016/j.scitotenv.2022.154833.
- Doong, D.J., Lo, W., Vojinovic, Z., Lee, W.L., Lee, S.P., 2016. Development of a new generation of flood inundation maps—a case study of the coastal city of Tainan, Taiwan. Water 8 (11), 521, https://doi.org/10.3390/W8110521.
- Eyring, V., Bony, S., Meehl, G.A., Senior, C.A., Stevens, B., Stouffer, R.J., Taylor, K.E., 2016. Overview of the Coupled Model Intercomparison Project Phase 6 (CMIP6) experimental design and organization. Geosci. Model Dev. 9 (5) https://doi.org/10.5194/gmd-9-1937-2016.
- Fang, X., Kuo, Y.H., Wang, A., 2011. The impacts of Taiwan topography on the predictability of typhoon Morakot's record-breaking rainfall: a high-resolution ensemble simulation. Weather Forecast. 26 (5), 613–633. https://doi.org/10.1175/WAF-D-10-05020.1.
- Fleischmann, A., Collischonn, W., Paiva, R., Tucci, C.E., 2019. Modeling the role of reservoirs versus floodplains on large-scale river hydrodynamics. Nat. Hazards 99 (2). https://doi.org/10.1007/s11069-019-03797-9.
- Ghosh, T.K., Jakobsen, F., Joshi, M., Pareta, K., 2019. Extreme rainfall and vulnerability assessment: case study of Uttarakhand rivers. Nat. Hazards 99 (2), 665–687. https://doi.org/10.1007/S11069-019-03765-3/TABLES/10.
- Gudmundsson, L., Boulange, J., Do, H.X., Gosling, S.N., Grillakis, M.G., Koutroulis, A.G., Leonard, M., Liu, J., Schmied, H.M., Papadimitriou, L., Pokhrel, Y., Seneviratne, S.I., Satoh, Y., Thiery, W., Westra, S., Zhang, X., Zhao, F., 2021. Globally observed trends in mean and extreme river flow attributed to climate change. Science 371 (6534). https://doi.org/10.1126/science.aba3996.
- Gupta, H.V., Kling, H., Yilmaz, K.K., Martinez, G.F., 2009. Decomposition of the mean squared error and NSE performance criteria: implications for improving hydrological modelling. J. Hydrol. 377 (1–2) https://doi.org/10.1016/j.jhydrol.2009.08.003.
- Hersbach, H., Bell, B., Berrisford, P., Hirahara, S., Horányi, A., Muñoz-Sabater, J., Nicolas, J., Peubey, C., Radu, R., Schepers, D., Simmons, A., Soci, C., Abdalla, S., Abellan, X., Balsamo, G., Bechtold, P., Biavati, G., Bidlot, J., Bonavita, M., Thépaut, J.N., et al., 2020. The ERA5 global reanalysis. Q. J. R. Meteorol. Soc. 146 (730) https://doi.org/10.1002/qj.3803.
- Hirabayashi, Y., Mahendran, R., Koirala, S., Konoshima, L., Yamazaki, D., Watanabe, S., Kim, H., Kanae, S., 2013. Global flood risk under climate change. Nat. Clim. Change 3 (9). https://doi.org/10.1038/nclimate1911.
- Hirabayashi, Y., Tanoue, M., Sasaki, O., Zhou, X., Yamazaki, D., 2021. Global exposure to flooding from the new CMIP6 climate model projections. Sci. Rep. 11 (1) https://doi.org/10.1038/s41598-021-83279-w.
- Hölbling, D., Friedl, B., Eisank, C., 2015. An object-based approach for semi-automated landslide change detection and attribution of changes to landslide classes in northern Taiwan. Earth Sci. Inform. 8 (2) https://doi.org/10.1007/s12145-015-0217-3.
- Hong, J.S., Fong, C.T., Hsiao, L.F., Yu, Y.C., Tzeng, C.Y., 2015. Ensemble typhoon quantitative precipitation forecasts model in Taiwan. Weather Forecast. 30 (1) https://doi.org/10.1175/WAF-D-14-00037.1.
- Hsiao, S.C., Chen, H., Wu, H.L., Chen, W.B., Chang, C.H., Guo, W.D., Chen, Y.M., Lin, L.Y., 2020. Numerical simulation of large wave heights from Super Typhoon Nepartak (2016) in the eastern waters of Taiwan. J. Mar. Sci. Eng. 8 (3) https://doi.org/10.3390/jmse8030217.
- Hsu, N.Y., Chen, P.Y., Chang, H.W., Su, H.J., 2011. Changes in profiles of airborne fungi in flooded homes in southern Taiwan after Typhoon Morakot. Sci. Total Environ. 409 (9) https://doi.org/10.1016/j.scitotenv.2011.01.042.
- Hsu, H., Dirmeyer, P.A., 2023. Uncertainty in projected critical soil moisture values in CMIP6 affects the interpretation of a more moisture-limited world. Earth's Future 11 (6), e2023EF003511. https://doi.org/10.1029/2023EF003511.
- Huang, W.C., Chang, T.H., Yang, F.T., 2001. Water supply evaluation of Taiwan's Silicon Valley. J. Am. Water Resour. Assoc. 37 (5) https://doi.org/10.1111/j.1752-1688.2001.tb03638.x.

- Huang, W.K., Wang, J.J., 2015. Typhoon damage assessment model and analysis in Taiwan. Nat. Hazards 79 (1). https://doi.org/10.1007/s11069-015-1858-8. Hung, C.W., Shih, M.F., Lin, T.Y., 2020. The climatological analysis of typhoon tracks, steering flow, and the pacific subtropical high in the vicinity of Taiwan and the Western North Pacific. Atmosphere 11 (5). https://doi.org/10.3390/atmos11050543.
- Huntington, T.G., 2006. Evidence for intensification of the global water cycle: review and synthesis. J. Hydrol. 319 (1-4), 83-95. https://doi.org/10.1016/J. JHYDROL. 2005.07.003
- Hussain, F., Wu, R.S., Yu, K.C., 2021. Application of physically based semi-distributed hec-hms model for flow simulation in tributary catchments of Kaohsiung area taiwan. J. Mar. Sci. Technol. 29 (1) https://doi.org/10.51400/2709-6998.1003.
- IPCC, 2024. Climate Change 2021 The Physical Science Basis. Cambridge University Press (In Press).
- Ji, L., Gong, P., Wang, J., Shi, J., Zhu, Z., 2018. Construction of the 500-m Resolution Daily Global Surface Water Change Database (2001–2016). Water Resour. Res. 54 (12), 10270–10292. https://doi.org/10.1029/2018WR023060.
- Kimura, N., Chiang, S., Cheng, C.-T., Wei, H.-P., Su, Y.-F., Chu, J.-L., Liou, J.-J., Chen, Y.-M., Lin, L.-Y., Wei, P., Su, Y.F., Chu, J.L., Cheng, C.T., Liou, J.J., Chen, Y.M., Lin, L.Y., 2014. Tsengwen reservoir watershed hydrological flood simulation under global climate change using the 20 km mesh meteorological research institute atmospheric general circulation model (MRI-AGCM). Terr. Atmos. Ocean. Sci. 25 (3), 449–461. https://doi.org/10.3319/TAO.2014.01.02.01(Hy).
- King, A.D., Pitman, A.J., Henley, B.J., Ukkola, A.M., Brown, J.R., 2020. The role of climate variability in Australian drought. Nat. Clim. Change 10 (3). https://doi.org/10.1038/s41558-020-0718-z.
- Knoben, W.J.M., Freer, J.E., Woods, R.A., 2019. Technical note: inherent benchmark or not? Comparing Nash-Sutcliffe and Kling-Gupta efficiency scores. Hydrol. Earth Syst. Sci. 23 (10), 4323–4331. https://doi.org/10.5194/HESS-23-4323-2019.
- Kuo, W.-P., 2019. Living with "abnormal" drought in rain-soaked Taiwan: analysis of water consumption practices and discourses. Anthropol. Noteb. 25 (2). (http://notebooks.drustvo-antropologov.si/Notebooks/article/view/25).
- Lee, C.S., Huang, L.R., Shen, H.S., Wang, S.T., 2006. A climatology model for forecasting typhoon rainfall in Taiwan. Nat. Hazards 37 (1–2). https://doi.org/10.1007/s11069-005-4658-8.
- Lee, C.H., Lin, S.H., Kao, C.L., Hong, M.Y., Huang, P.C., Shih, C.L., Chuang, C.C., 2020. Impact of climate change on disaster events in metropolitan cities-trend of disasters reported by Taiwan national medical response and preparedness system. Environ. Res. 183 https://doi.org/10.1016/j.envres.2020.109186.
- Lee, C.H., Yeh, H.F., 2019. Impact of climate change and human activities on streamflow variations based on the Budyko framework. Water 11 (10), 2001. https://doi.org/10.3390/W11102001.
- Lehner, F., Wood, A.W., Vano, J.A., Lawrence, D.M., Clark, M.P., Mankin, J.S., 2019. The potential to reduce uncertainty in regional runoff projections from climate models. Nat. Clim. Change 9 (12). https://doi.org/10.1038/s41558-019-0639-x.
- Li, X., Fu, D., Nielsen-Gammon, J., Gangrade, S., Kao, S.C., Chang, P., Morales Hernández, M., Voisin, N., Zhang, Z., Gao, H., 2023. Impacts of climate change on future hurricane induced rainfall and flooding in a coastal watershed: a case study on Hurricane Harvey. J. Hydrol. 616 https://doi.org/10.1016/j.ihydrol.2022.128774.
- Li, M.H., Yang, M.J., Soong, R., Huang, H.L., 2005. Simulating Typhoon floods with gauge data and mesoscale-modeled rainfall in a mountainous watershed. J. Hydrometeorol. 6 (3), 306–323. https://doi.org/10.1175/JHM423.1.
- Lin, Y.P., Lin, Y.Bin, Wang, Y.T., Hong, N.M., 2008. Monitoring and predicting land-use changes and the hydrology of the urbanized Paochiao watershed in Taiwan using remote sensing data, urban growth models and a hydrological model. Sensors 8 (2). https://doi.org/10.3390/s8020658.
- Lin, C.H., Lin, M.L., 2015. Evolution of the large landslide induced by Typhoon Morakot: a case study in the Butangbunasi River, southern Taiwan using the discrete element method. Eng. Geol. 197 https://doi.org/10.1016/j.enggeo.2015.08.022.
- Liu, W.-C., Hsieh, T.-H., Liu, H.-M., Flood Risk Assessment in, H., Rosen, M.A., Bathrellos, G.D., 2021. Flood risk assessment in urban areas of southern Taiwan. Sustainability 13 (6), 3180. https://doi.org/10.3390/SU13063180.
- Liu, X., Yuan, X., Ma, F., Xia, J., 2023. The increasing risk of energy droughts for hydropower in the Yangtze River basin. J. Hydrol. 621, 129589 https://doi.org/10.1016/L.JHYDROL.2023.129589.
- Ourbak, T., Magnan, A.K., 2018. The Paris Agreement and climate change negotiations: small Islands, big players. Reg. Environ. Change 18 (8). https://doi.org/
- Patz, J.A., Campbell-Lendrum, D., Holloway, T., Foley, J.A., 2005. Impact of regional climate change on human health. Nature 438 (7066). https://doi.org/10.1038/
- Payne, A.E., Demory, M.E., Leung, L.R., Ramos, A.M., Shields, C.A., Rutz, J.J., Siler, N., Villarini, G., Hall, A., Ralph, F.M., 2020. Responses and impacts of atmospheric rivers to climate change. Nat. Rev. Earth Environ. 1 (3) https://doi.org/10.1038/s43017-020-0030-5.
- Pekel, J.F., Cottam, A., Gorelick, N., Belward, A.S., 2016. High-resolution mapping of global surface water and its long-term changes. Nature 540 (7633). https://doi.org/10.1038/nature20584.
- Pokhrel, Y., Burbano, M., Roush, J., Kang, H., Sridhar, V., Hyndman, D.W., 2018a. A review of the integrated effects of changing climate, land use, and dams on Mekong river hydrology. Water 10 (3). https://doi.org/10.3390/W10030266.
- Pokhrel, Y., Felfelani, F., Satoh, Y., Boulange, J., Burek, P., Gädeke, A., Gerten, D., Gosling, S.N., Grillakis, M., Gudmundsson, L., Hanasaki, N., Kim, H., Koutroulis, A., Liu, J., Papadimitriou, L., Schewe, J., Müller Schmied, H., Stacke, T., Telteu, C.E., Wada, Y., et al., 2021. Global terrestrial water storage and drought severity under climate change. Nat. Clim. Change 11 (3). https://doi.org/10.1038/s41558-020-00972-w.
- Pokhrel, Y., Hanasaki, N., Koirala, S., Cho, J., Yeh, P.J.F., Kim, H., Kanae, S., Oki, T., 2012. Incorporating anthropogenic water regulation modules into a land surface model. J. Hydrometeorol. 13 (1) https://doi.org/10.1175/JHM-D-11-013.1.
- Pokhrel, Y., Hanasaki, N., Wada, Y., Kim, H., 2016. Recent progresses in incorporating human land–water management into global land surface models toward their integration into Earth system models. Wiley Interdiscip. Rev.: Water 3 (4). https://doi.org/10.1002/wat2.1150.
- Pokhrel, Y., Koirala, S., Yel, P.J.F., Hanasaki, N., Longuevergne, L., Kanae, S., Oki, T., 2015. Incorporation of groundwater pumping in a global land surface model with the representation of human impacts. Water Resour. Res. 51 (1), 78–96. https://doi.org/10.1002/2014WR015602.
- Pokhrel, Y., Shin, S., Lin, Z., Yamazaki, D., Qi, J., 2018b. Potential disruption of flood dynamics in the Lower Mekong River Basin due to upstream flow regulation. Sci. Rep. 8 (1), 1–13. https://doi.org/10.1038/s41598-018-35823-4.
- Pokhrel, Y., Shin, S., Lin, Z., Yamazaki, D., Qi, J., 2018c. Potential disruption of flood dynamics in the Lower Mekong river basin due to upstream flow regulation. Sci. Rep. 8 (1) https://doi.org/10.1038/S41598-018-35823-4.
- Rasiah, R., Shahrivar, R.B., Yap, X.S., 2016. Institutional support, innovation capabilities and exports: evidence from the semiconductor industry in Taiwan. Technol. Forecast. Soc. Change 109. https://doi.org/10.1016/j.techfore.2016.05.015.
- Ripple, W.J., Wolf, C., Gregg, J.W., Levin, K., Rockström, J., Newsome, T.M., Betts, M.G., Huq, S., Law, B.E., Kemp, L., Kalmus, P., Lenton, T.M., 2022. World scientists' warning of a climate emergency 2022. BioScience 72 (12). https://doi.org/10.1093/biosci/biac083.
- Satoh, Y., Yoshimura, K., Pokhrel, Y., Kim, H., Shiogama, H., Yokohata, T., Hanasaki, N., Wada, Y., Burek, P., Byers, E., Schmied, H.M., Gerten, D., Ostberg, S., Gosling, S.N., Boulange, J.E.S., Oki, T., 2022. The timing of unprecedented hydrological drought under climate change. Nat. Commun. 13 (1) https://doi.org/10.1038/s41467-022-30729-2.
- Shieh, C.-L., Wang, C.-M., Chen, Y.-S., Tsai, Y.-J., Tseng, W.-H., 2010. An overview of disasters resulted from Typhoon Morakot in Taiwan. J. Disaster Res. 5, 236–244. (https://www.researchgate.net/publication/285977880).
- Shih, D.S., Chen, C.H., Yeh, G.T., 2014. Improving our understanding of flood forecasting using earlier hydro-meteorological intelligence. J. Hydrol. 512 https://doi.org/10.1016/j.jhydrol.2014.02.059.
- Shih, H.J., Chen, H., Liang, T.Y., Fu, H.S., Chang, C.H., Chen, W.B., Su, W.R., Lin, L.Y., 2018. Generating potential risk maps for typhoon-induced waves along the coast of Taiwan. Ocean Eng. 163 https://doi.org/10.1016/j.oceaneng.2018.05.045.
- Shin, S., Pokhrel, Y., Talchabhadel, R., Panthi, J., 2021. Spatio-temporal dynamics of hydrologic changes in the Himalayan river basins of Nepal using high-resolution hydrological-hydrodynamic modeling. J. Hydrol. 598, 126209 https://doi.org/10.1016/J.JHYDROL.2021.126209.

- Shin, S., Pokhrel, Y., Yamazaki, D., Huang, X., Torbick, N., Qi, J., Pattanakiat, S., Ngo-Duc, T., Nguyen, T.D., 2020a. High resolution modeling of river-floodplain-reservoir inundation dynamics in the Mekong River basin. Water Resour. Res. 56 (5) https://doi.org/10.1029/2019WR026449.
- Shin, S., Pokhrel, Y., Yamazaki, D., Huang, X., Torbick, N., Qi, J., Pattanakiat, S., Ngo-Duc, T., Nguyen, T.D., 2020b. High resolution modeling of river-floodplain-reservoir inundation dynamics in the Mekong River basin. Water Resour. Res. 56 (5), e2019WR026449 https://doi.org/10.1029/2019WR026449.
- Sui, C.H., Huang, C.Y., Tsai, Y.Ben, Chen, C.Sen, Lin, P.L., Shieh, S.L., Li, M.H., Liou, Y.A., Wang, T.C.C., Wu, R.S., Liu, G.R., Ch, Y.H., 2002. Meteorology-hydrology study targets Typhoon Nari and Taipei flood. Eos 83 (24). https://doi.org/10.1029/2002E0000186.
- Takata, K., Emori, S., Watanabe, T., 2003. Development of the minimal advanced treatments of surface interaction and runoff. Glob. Planet. Change 38 (1–2). https://doi.org/10.1016/S0921-8181(03)00030-4.
- Tang, C.H., Hsu, Y.J., Barbot, S., Moore, J.D.P., Chang, W.L., 2019. Lower-crustal rheology and thermal gradient in the Taiwan orogenic belt illuminated by the 1999 Chi-Chi earthquake. Sci. Adv. 5 (2) https://doi.org/10.1126/SCIADV.AAV3287/SUPPL FILE/AAV3287 SM.PDF.
- Tang, X.D., Yang, M.J., Tan, Z.M., 2012. A modeling study of orographic convection and mountain waves in the landfalling typhoon Nari (2001). Q. J. R. Meteorol. Soc. 138 (663) https://doi.org/10.1002/qj.933.
- Tsao, J., Lee, C.H., Yel, H.F., 2020. Attribution of Streamflow Variations in Southern Taiwan. Water 12 (9), 2465. https://doi.org/10.3390/W12092465.
- Tsou, C.Y., Feng, Z.Y., Chigira, M., 2011. Catastrophic landslide induced by Typhoon Morakot, Shiaolin, Taiwan. Geomorphology 127 (3–4), 166–178. https://doi.org/10.1016/J.GEOMORPH.2010.12.013.
- Warszawski, L., Frieler, K., Huber, V., Piontek, F., Serdeczny, O., Schewe, J., 2014. The inter-sectoral impact model intercomparison project (ISI-MIP): project framework. Proc. Natl. Acad. Sci. USA 111 (9). https://doi.org/10.1073/pnas.1312330110.
- Weedon, G.P., Balsamo, G., Bellouin, N., Gomes, S., Best, M.J., Viterbo, P., 2014. The WFDEI meteorological forcing data set: WATCH Forcing data methodology applied to ERA-Interim reanalysis data. Water Resour. Res. 50 (9) https://doi.org/10.1002/2014WR015638.
- Wei, H.P., Li, H.C., Yeh, K.C., Liou, J.J., Chen, Y.M., Lin, H.J., 2016. Using structural measures to reduce flood losses in a future extreme weather event. Terr. Atmos. Ocean. Sci. 27 (5) https://doi.org/10.3319/TAO.2016.07.14.02.
- Wei, H.P., Yeh, K.C., Liou, J.J., Chen, Y.M., Cheng, C.T., 2016. Estimating the risk of river flow under climate change in the Tsengwen River basin. Water 8 (3), 81. https://doi.org/10.3390/W8030081.
- Wu, C.H., Chen, S.C., Feng, Z.Y., 2014. Formation, failure, and consequences of the Xiaolin landslide dam, triggered by extreme rainfall from Typhoon Morakot, Taiwan. Landslides 11 (3). https://doi.org/10.1007/s10346-013-0394-4.
- Yamazaki, D., De Almeida, G.A.M., Bates, P.D., 2013. Improving computational efficiency in global river models by implementing the local inertial flow equation and a vector-based river network map. Water Resour. Res. 49 (11) https://doi.org/10.1002/wrcr.20552.
- Yamazaki, D., Ikeshima, D., Sosa, J., Bates, P., Allen, G., Pavelsky, T., 2019. MERIT hydro: a high-resolution global hydrography map based on latest topography dataset. Water Resour. Res. 55 (6) https://doi.org/10.1029/2019WR024873.
- Yamazaki, D., Kanae, S., Kim, H., Oki, T., 2011. A physically based description of floodplain inundation dynamics in a global river routing model. Water Resour. Res. 47 (4) https://doi.org/10.1029/2010WR009726.
- Yamazaki, D., Lee, H., Alsdorf, D.E., Dutra, E., Kim, H., Kanae, S., Oki, T., Yamazaki, C., Lee, H., Alsdorf, D.E., Dutra, E., Kim, H., Kanae, S., Oki, T., 2012. Analysis of the water level dynamics simulated by a global river model: a case study in the Amazon River. Water Resour. Res. 48 (9), 9508. https://doi.org/10.1029/2012WR011869.
- Yamazaki, D., Sato, T., Kanae, S., Hirabayashi, Y., Bates, P.D., 2014. Regional flood dynamics in a bifurcating mega delta simulated in a global river model. Geophys. Res. Lett. 41 (9) https://doi.org/10.1002/2014GL059744.
- Yang, T.H., Yang, S.C., Ho, J.Y., Lin, G.F., Hwang, G.Do, Lee, C.S., 2015. Flash flood warnings using the ensemble precipitation forecasting technique: a case study on forecasting floods in Taiwan caused by typhoons. J. Hydrol. 520, 367–378. https://doi.org/10.1016/J.JHYDROL.2014.11.028.
- Yang, M.J., Zhang, D.L., Huang, H.L., 2008. A modeling study of Typhoon Nari (2001) at landfall. Part I: Topographic effects. J. Atmos. Sci. 65 (10), 3095–3115. https://doi.org/10.1175/2008JAS2453.1.
- Yeh, H.F., 2019. Using integrated meteorological and hydrological indices to assess drought characteristics in southern Taiwan. Hydrol. Res. 50 (3) https://doi.org/10.2166/nb.2019.120.
- Yeh, H.F., Tsao, J., 2020. Hydrological response to natural and anthropogenic factors in Southern Taiwan. Sustainability 12 (5), 1981. https://doi.org/10.3390/
- Yeh, C.F., Wang, J., Yeh, H.F., Lee, C.H., 2015. Spatial and temporal streamflow trends in Northern Taiwan. Water 7 (2), 634–651. https://doi.org/10.3390/ W7020634
- Yen, J.H., Chen, C.Y., 2001. Allocation strategy analysis of water resources in South Taiwan. Water Resour. Manag. 15 (5) https://doi.org/10.1023/A: 1014441319406.
- Yu, P.S., Yang, T.C., Kuo, C.C., 2006. Evaluating long-term trends in annual and seasonal precipitation in Taiwan. Water Resour. Manag. 20 (6), 1007–1023. https://doi.org/10.1007/S11269-006-9020-8/METRICS.
- Zhao, F., Veldkamp, T.I.E., Frieler, K., Schewe, J., Ostberg, S., Willner, S., Schauberger, B., Gosling, S.N., Schmied, H.M., Portmann, F.T., Leng, G., Huang, M., Liu, X., Tang, Q., Hanasaki, N., Biemans, H., Gerten, D., Satoh, Y., Pokhrel, Y., Yamazaki, D., et al., 2017. The critical role of the routing scheme in simulating peak river discharge in global hydrological models. Environ. Res. Lett. 12 (7) https://doi.org/10.1088/1748-9326/aa7250.